Modeling the contribution of quantum confinement to luminescence from silicon nanoclusters

P. F. Trwoga,[a] A. J. Kenyon,[b] and C. W. Pitt

Department of Electronic and Electrical Engineering, University College London, Torrington Place, London WC1E 7JE, United Kingdom

(Received 8 September 1997; accepted for publication 15 December 1997)

We present a model for the luminescence spectrum of silicon nanoclusters. We propose that the major contribution to luminescence is from radiative recombination of confined excitons (quantum confinement). Utilizing the effective mass approximation we consider the variation in oscillator strength with cluster size and the associated change in the number of available free carriers. By varying both the mean cluster size and size distribution of silicon nanoclusters, the luminescence spectra are modeled to a good fit. We compare our model with experimental photoluminescence and electroluminescence data from this group and from others. © *1998 American Institute of Physics.* [S0021-8979(98)00307-7]

I. INTRODUCTION

Confined silicon systems are of interest because they offer the possibility of light emission from silicon-based material and devices. Following the initial report by Canham in 1990[1] of light emission from porous silicon, this and other confined systems have been the subject of intense scientific activity. A number of schemes have been proposed to account for the observed luminescence; these include quantum confinement of excitons, luminescence from chemical species such as siloxenes, interfacial states, defects, and strain related luminescence.[2–5] However, there is a growing consensus that quantum confinement effects can explain the majority of the observed luminescence spectra.[2,6] While it is clear that, in some cases at least, other mechanisms are present, we have set out in this study to investigate what might be the contribution from confinement effects taken in isolation.

A. Quantum mechanical background of confined systems

In its most general form a confined system is one in which a particle (in this case an electron) is held in a potential well bounded by high and wide potential barriers. Quantum confinement effects arise when the confinement dimension is of the order of the period of the wave function of the confined particle. In a confined system the energy of the allowable electronic states increases with the degree of confinement. The familiar result is that the energy is quantized into eigenvalues that make up the energy levels of the system given by

$$E_n = \frac{n^2 \pi^2 h^2}{2mR^2} \tag{1}$$

for $n = 1, 2, 3...$, m is the particle mass, and R is the width of the well within which the particle is confined.

Quantum confinement effects are only significant for systems in which the Bohr radius of the exciton is of the order of, or larger than, the size of the confined system. In a semiconductor the most immediate consequence of the confinement effect is an increase in the band gap energy and an associated increased probability of radiative transfer. As the carriers are confined in real space, their associated wave functions spread out in momentum space. This increases the probability of radiative transitions as the electron-hole wave function overlap is greater. In the case of silicon, although the band gap remains indirect for all but the smallest clusters, scattering of the confined exciton at the cluster boundaries by incident photons or electrons can supply the required momentum for the indirect transition.

Three distinct categories of confinement can be identified, strong, medium, and weak, according to the relative sizes of the Bohr radius and the potential well. The weak confinement regime is that in which R is greater than the bulk exciton Bohr radius a_B. Moderate confinement regimes exist where the excitonic Bohr radius and the size of the cluster are roughly equal, and $a_h < R < a_e$ where a_h and a_e are the hole and electron Bohr radii, respectively. The strong confinement regime is that in which $R < a_B$ and $R < a_h, a_e$. In this case the energy levels of the excitons become discrete rather than bands.

The values of the Bohr radii of electron, hole, and exciton are given by

$$a_e = \frac{4\pi h^2 \epsilon_r \epsilon_0}{m_e^* e^2}, \tag{2a}$$

$$a_h = \frac{4\pi h^2 \epsilon_r \epsilon_0}{m_h^* e^2}, \tag{2b}$$

$$a_b = \frac{4\pi h^2 \epsilon_r \epsilon_0}{\mu e^2}, \tag{2c}$$

m_e^* and m_h^* being the effective mass of the electron and hole, respectively, μ the reduced mass, and ϵ_r the relative permittivity.

[a] Electronic mail: p.trwoga@eleceng.ucl.ac.uk
[b] Electronic mail: t.kenyon@eleceng.ucl.ac.uk

Since the effective mass is directly related to the gradient of the $E-k$ curve, the effective mass of the hole and electron will be different in the confined system compared to the bulk. For Si clusters these quantities have been estimated by Xia[7] and Yoffe[8] to be $m_e^* = 0.19 \, m_0$ and $m_h^* = 0.286 \, m_0$. This gives values for the Bohr radii of $a_e = 3.19 \times 10^{-9}$, $a_h = 2.11 \times 10^{-9}$, and $a_B = 5.30 \times 10^{-9}$ m.

The sizes of the Si clusters grown at University College London (UCL) have been estimated from a comparison of the peak luminescence energy with the predicted energy gap E_g which was in turn derived from a theoretical study with good agreement with experimental data.[9] This suggests a typical size of 20 Å as grown and up to 40 Å following high temperature annealing. Thus the material grown by plasma enhanced chemical vapor deposition (PECVD) in our laboratory is clearly in the strong confinement regime (20–40 Å).

B. Quantum confinement in semiconductors: Theory and experimental evidence

Some experimental evidence for quantum size effects in confined excitons was obtained by Ekimov and Onushchenko[10] in 1981. The experiment involved production of ~30 Å CuCl crystallites dispersed in a silicate glass, and the observation of a blueshift in the main exciton absorption. This work led to the first real treatment of this subject by Efros and Efros[11] in 1982. Their model was based on the effective mass approximation (EMA) with parabolic energy bands and assumed spherical microcrystallites with infinite potential barriers at the crystallite boundary. R was replaced with $\bar{R}$, the average crystal size.

In the weak confinement regime the dominant energy term is the Coulomb term, and quantization of the motion of the exciton occurs. The shift in energy of the lowest energy state is

$$\Delta E \approx \frac{h^2 \pi^2}{2M \bar{R}^2} \quad \text{(weak confinement)}, \tag{3}$$

where M is the mass of the exciton and is given by $M = m_e^* + m_h^*$.

In the strong confinement case, the Coulomb term turns out to be small and can be ignored. The electrons and holes can now be thought of as independent particles; excitons are not formed. Separate quantization of motion of the electron and hole is now an important factor. The optical spectra should consist of a series of lines due to transitions between subbands. The shift in energy is now

$$\Delta E \approx \frac{h^2 \pi^2}{2\mu \bar{R}^2} \quad \text{(strong confinement)}, \tag{4}$$

where the excitonic mass is now replaced by the reduced mass μ.

For very small clusters there is a large difference between the effective mass of the electron and the much heavier hole. The reduced mass μ can now be replaced with m_e^*. It is now the electron behavior that is confined and the hole interacts through the Coulomb potential.

$$\Delta E \approx \frac{h^2 \pi^2}{2 m_e^* \bar{R}^2} \quad \text{(very small nanoclusters)}. \tag{5}$$

Since the original analysis of Efros and Efros in 1982 several other models have been developed with various refinements.

The effective mass approximation is idealized by assuming the cluster to be in an infinite potential well and by excluding the Coulomb terms from the analysis. Brus in 1984[12] enhanced the original model by including the Coulomb terms and considering the effect on the exciton binding energy of the dielectric constant of the matrix, and employed finite potential wells to calculate the energy states. Other EMA models were developed by Kayanuma[13] and Kayanuma and Momiji[14] which used finite potentials to treat spherical and cylindrical clusters.

The empirical tight binding method (ETBM) employs nonparabolic energy bands away from the Brillouin zone center. This model was developed in 1991 by Wang and Herron[15] and uses experimentally obtained fitting parameters. Other models have been developed that are more specific to particular semiconductor systems such as the empirical pseudopotential method (EPM)[16] and the effective bond order model (EBOM) which includes modifications for II–VI semiconductors.[17] The EPM is not a first principle model but is a reliable technique that agrees well with experiment. EBOM is semiempirical but uses the EMA to model the conduction band and the ETBM to model the valence band. This model is known to overestimate exciton energies.

The extension of the Efros and Efros model by Brus and by Kayanuma to include Coulomb and correlation energy terms enables derivation of an expression that models energies and provides a reasonable guide to cluster size as a function of E_g.

$$E(R) = E_g + \frac{h^2 \pi^2}{2R^2}\left(\frac{1}{m_e^*} + \frac{1}{m_h^*}\right) - \frac{1.786 e^2}{\epsilon_r R} + 0.284 \; E_R, \tag{6}$$

where E_R is the Rydberg energy for the bulk semiconductor:

$$E_R = \left(\frac{13.606 \; m_0}{\epsilon_r^2 (1/m_e^* + 1/m_h^*)}\right) \text{eV}; \tag{7}$$

$1.786 \; e^2/\epsilon_r R$ is the Coulomb term and $0.248 \; E_R$ gives the spatial correlation energy and is a minor correction. This method is known to overestimate the energy values $E(R)$, particularly for small clusters in the sub-20 Å range. More accurate models that use finite barriers give the relationship of the confined energy gap to the cluster size as $R \propto (1/\gamma)$ where γ is an empirically derived value in the range 1.3–1.8. However, in this study the first principle EMA relationship will be used to examine the general trend.

II. EXPERIMENT

We have proposed in previous work[18,19] that luminescence from silicon-rich silica produced by PECVD may be separated into two distinct bands. The lower energy of these we have ascribed to quantum confinement of excitons; the

higher energy band we propose to be due to the presence of nonbridging oxygen hole centers. Selection of appropriate growth parameters and suitable postprocessing allows the production of samples which exhibit only the lower energy band. These are the samples which we have used to provide experimental data against which to judge the success of our model.

It is inherent in the fabrication process of PECVD grown SiO_x that there will exist a distribution of cluster sizes that are centered around a mean size of diameter d_0. It was assumed in this study that the width of the luminescence line shape is dominated by the size dispersion of the clusters in the SiO_2 matrix. From early work by Lifshitz,[20] later work based on Lifshitz by Chen et al.,[21] and also from experimental data on size distribution[22] it is a reasonable assumption that the Si cluster sizes are dispersed in a normal distribution P_d, represented by

$$P_d = \frac{1}{\sqrt{2\pi}\sigma}\exp\left(-\frac{(d-d_0)^2}{2\sigma^2}\right), \tag{8}$$

where d is the cluster diameter and σ is the standard deviation.

The issue of the effect of the change in oscillator strength with d has been addressed by Khurgin et al.[23] If only spherical silicon clusters are considered, oscillator strength will increase with decreasing cluster size according to

$$f \approx \left(\frac{\sin(0.86\pi d/a)}{[1-(0.86\pi d_s/a)]\times 0.86\pi d_s/a}\right), \tag{9}$$

where a is the lattice constant (5.43 Å for bulk silicon) and d_s is in this case the diameter of the cluster but this relationship also applies to the smallest dimension of an irregular crystallite. This implies that small clusters will make a disproportionally large contribution to the luminescence spectrum and cause a deviation from a Guassian luminescence line shape. The above equation contains a sine function that leads to oscillations; this appears to be an artifact of the assumptions made in the derivation; the dips to zero have no physical meaning. For the purpose of the model the overall oscillator strength f was further approximated by a power law as

$$f \propto d^{-2.25}. \tag{10}$$

The diameter d can be then substituted for the energy shift ΔE:

$$f(\Delta E) = 0.15\Delta E^{2.25}. \tag{11}$$

The number of carriers N_c will increase as the cluster size increases; for large clusters more carriers are available to take part in optical transitions. The number of carriers available in a cluster scales with cluster diameter as

$$N_c \propto d^3. \tag{12}$$

Chen et al.[21] have studied the effect of size distribution on photoluminescence spectra for Si nanoclusters and derived a relationship for the photoluminescence spectrum for quan-
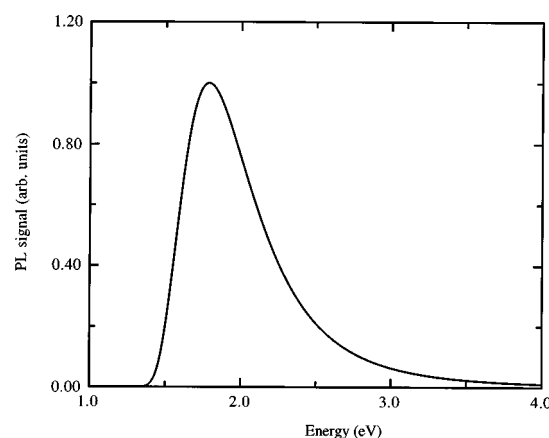

FIG. 1. Simulated spectrum for a sample having a mean cluster size of 40 Å and 10% size dispersion.

tum confinement of clusters that takes into account the increase in electron-holes pairs with increasing size:

$$P(\Delta E) = \frac{K}{\Delta E^3}\exp\left\{-\frac{1}{2}\left(\frac{d_0}{\sigma}\right)^2\left[\left(\frac{\Delta E_0}{\Delta E}\right)^{1/2}-1\right]^2\right\}, \tag{13}$$

where K is a normalization constant.

The cubic term required to compensate for decreasing number of carriers with decreasing cluster size is taken care of in the pre-exponential term of this equation. The spectrum $S(\Delta E)$ can be thus represented by

$$S(\Delta E) = P(\Delta E)\times f(\Delta E). \tag{14}$$

It is instructive to compare this model with experimental data for Si clusters fabricated by various techniques. Care was taken to select experimental samples which were free from defect-related luminescence. In the case of UCL data, samples were selected which had been annealed at 1000 °C and they exhibited appropriately clear spectra. At this temperature, the majority of defects is removed and the remaining luminescence band centered around 1.6 eV has been assigned to quantum confinement effects.[18] Non-UCL data were selected on the basis of an absence of the 2–2.2 eV
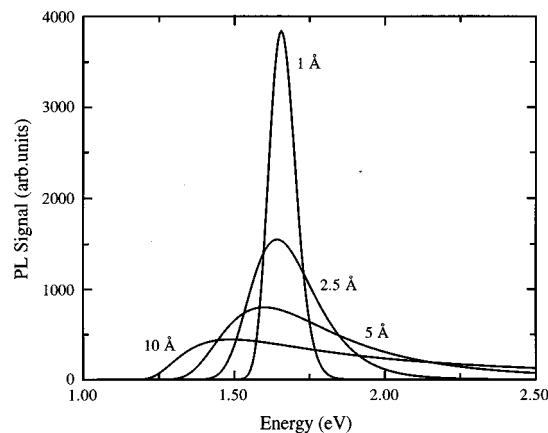

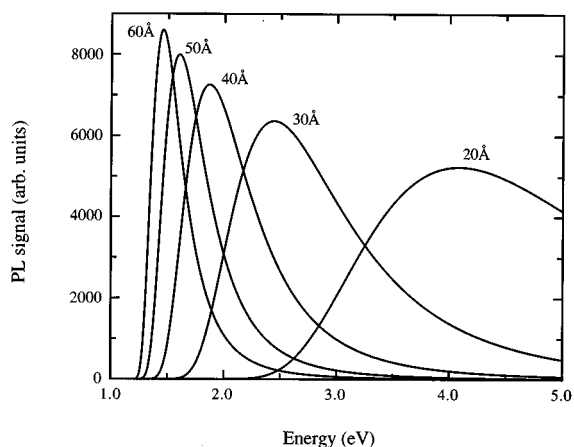FIG. 2. The effect of changing cluster size distribution.

FIG. 3. Luminescence spectrum as a function of mean cluster size.

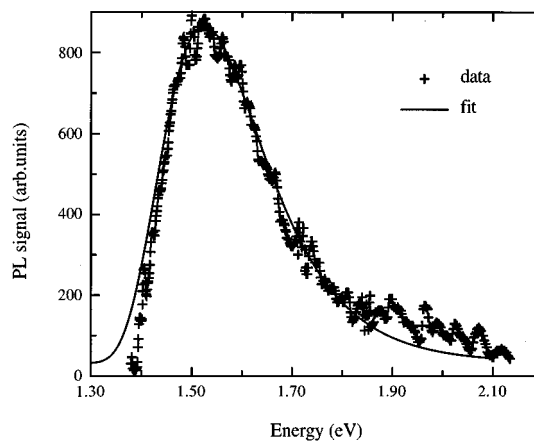FIG. 5. Fit to experimental photoluminescence data from Ghislotti *et al.* (after Ref. 24).

defect-related luminescence band. The experimental data in the case of non-UCL data have been accurately extracted using a scanner technique and give a true representation of the original published data.

III. RESULTS AND DISCUSSION

Figure 1 shows a typical modeled spectrum based on a mean cluster size of 40 Å and a standard deviation of 10%. This shows a marked deviation from the normal distribution at higher energies due to the increase in oscillator strength with decreasing cluster size.

Figure 2 shows photoluminescence as a function of cluster size dispersion; each photoluminescence spectrum shown has a mean cluster size of 50 Å. The peak position redshifts and the peak intensity reduces with an increase in the standard deviation. This highlights the tunability of this material and suggests that if the size dispersion could be somehow kept very low, intense photoluminescence from a narrow range of wavelength is possible.

Figure 3 shows the change in the modeled photolumines-

cence spectrum as the mean cluster size is changed. As expected, the luminescence peak blueshifts as the mean cluster size decreases. In addition, the spectrum becomes broader as the mean size becomes smaller due to the rapidly increasing oscillator strength at smaller dimensions. This plot again shows how these types of materials can be tuned to a particular peak wavelength through control of cluster size. Integration of the area under the photoluminescence curves shows that the overall quantum efficiency also increases as the size decreases. This is to be expected as a result of the increase in oscillator strength.

Figures 4, 5, 6, and 7 show experimental photoluminescence data from silicon-rich silica samples fitted using the full model. Figure 4 uses experimental data published by Zhang *et al.*[22] who quoted a mean cluster size of 55 Å. Figure 5 shows data published by Ghislotti *et al.*[24] while Figs. 6 and 7 use data obtained from films grown at UCL.

Table I details the important parameters derived from fitting the data. The fitting technique used was a Monte Carlo routine using around 3000 iterations for each fit.
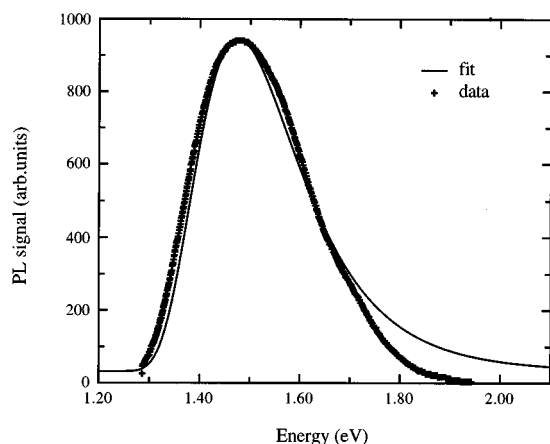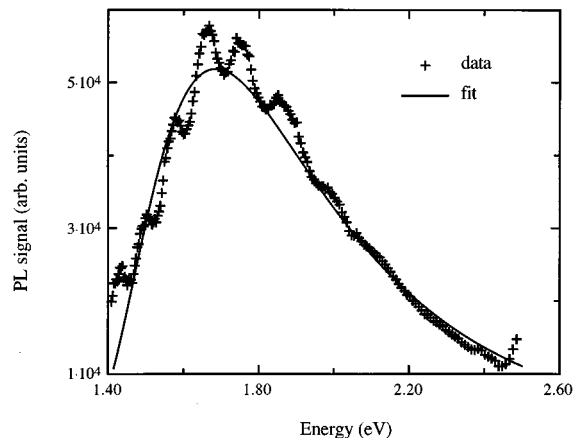

FIG. 4. Fit to experimental photoluminescence data from Zhang *et al.* (after Ref. 22).

FIG. 6. Fit to experimental photoluminescence data from UCL sample SS27 (1000 °C).

TABLE I. Fitting parameters obtained for each of the four samples studied.

Sample	Mean diameter (Å)	Std. dev. σ (Å)
Ghislotti et al.[a]	56.5	3.5
Zhang et al.[b]	60	4.2
UCL SS27 (1000 °C anneal)	45.4	5.1
UCL TEL2 (electroluminescence)	46.8	3.39

[a]Reference 24.
[b]Reference 22.

The Ghislotti data were well fitted by the model, although it slightly overestimated the ''bell'' part of the photoluminescence spectrum. The material used in this study was Si implanted SiO_2 layers annealed at 1000 °C in vacuum.

The Zhang data were from material fabricated by oxidizing silicon nanoparticles that were produced using a nonthermal microwave plasma gas phase process. This study actually provided a mean size for the unoxidized sample of 55 Å. The model appears to agree reasonably well with this value. From a histogram of particle sizes provided in Ref. 23 the standard deviation of the as-grown sample can be calculated to be around 38% of the mean. However this appears to change following the oxidizing process and the model indicates the standard deviation to be in the region of 4.5 Å, or 8.1% of the mean cluster diameter.

The details of the synthesis of the UCL samples have been reported previously.[18,19,25] However, it is informative to examine the photoluminescence data using the model described. The material consists of silicon nanoclusters embedded in a silica host. The photoluminescence data from sample SS27 were taken from a section of the film that was annealed at 1000 °C for 90 min. The data from TEL2 are an electroluminescence spectrum that is likely to be predominantly due to size effects, hence its inclusion in this study. The overall fit for these data is not as good as the other three; the tail in particular appears to be overestimated. The fitting was affected because data for only one side of the peak were available.

Most of the data is fitted well by the model but there is a scarcity of data for cluster size distributions available. The only measured mean size was from the Zhang data[22] (estimated from transmission electron microscopy studies) and this value was reasonably well confirmed by the model.

IV. CONCLUSIONS

The model developed for the photoluminescence of Si clusters is only concerned with luminescence as a result of recombination of confined excitons within Si nanoclusters. The EMA model is satisfactory as an approximate technique for estimating the modified band gap of the Si clusters over the size range 20–80 Å. Experimental evidence in the main indicates that the quantum confinement photoluminescence spectra deviate from a Gaussian distribution. This is most likely to be due to the increase in population of electron-hole pairs in larger clusters making a greater contribution to the
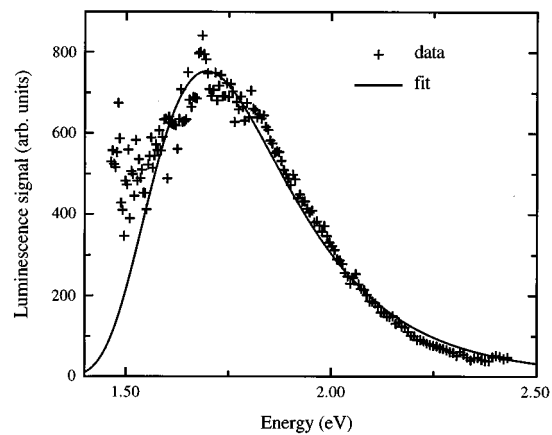

FIG. 7. Fit to electroluminescence data from UCL sample TEL2 (unannealed).

overall spectrum. The increase in oscillator strength, due to the reduction of size, further modifies the spectrum.

The inclusion of further corrections to the EMA model (increase in oscillator strength for decreasing cluster sizes and increase in numbers of electron-hole pairs for increasing cluster sizes) has carried with it some approximations and assumptions. In particular it appears that the oscillator strength term is too high and a more rigorous treatment using a larger spread of size distributions is needed. However, it is still useful to predict an approximate photoluminescence spectrum of Si clusters in a high band gap matrix such as SiO_2.

This work employed the effective mass approximation to calculate the band gap of silicon nanoclusters. It is known that this method overestimates the band gap energy for clusters smaller than 20 Å. However, this study has been limited to larger clusters in order to investigate the contribution to the luminescence spectrum of cluster size dispersion and the variation in oscillator strength. To further improve the model, a tight binding approximation for the calculation of band gap is being considered.

[1] L. T. Canham, Appl. Phys. Lett. **57**, 1046 (1990).
[2] L. T. Canham, Phys. Status Solidi B **190**, 9 (1995).
[3] B. H. Augustine, E. A. Irene, Y. J. He, K. J. Price, L. E. McNeil, K. N. Christensen, and D. M. Maher, J. Appl. Phys. **78**, 4020 (1995).
[4] Y. Kanemitsu, T. Ogawa, K. Shiraishi, and K. Takeda, Phys. Rev. B **48**, 4883 (1993).
[5] M. Stutzmann, M. S. Brandt, M. Rosenbauer, H. D. Fuchs, S. Finkbeiner, J. Weber, and P. Deak, J. Lumin. **57**, 321 (1993).
[6] R. T. Collins, P. M. Fauchet, and M. A. Tischler, Phys. Today **50**, 24 (1997).
[7] J. B. Xia, Phys. Rev. B **40**, 8500 (1989).
[8] A. D. Yoffe, Adv. Phys. **42**, 173 (1993).
[9] N. Hill and K. B. Whaley, Mater. Res. Soc. Symp. Proc. **358**, 25 (1995).
[10] A. I. Ekimov and A. A. Onushchenko, JETP Lett. **34**, 345 (1981).
[11] A. L. Efros and A. L. Efros, Sov. Phys. Semicond. **16**, 772 (1982).
[12] L. E. Brus, J. Lumin. **31**, 381 (1984).
[13] Y. Kayanuma, Phys. Rev. B **38**, 9797 (1988).

[14] Y. Kayanuma and H. Momiji, Phys. Rev. B **41**, 10 261 (1990).

[15] Y. Wang and N. Herron, J. Phys. Chem. **95**, 525 (1991).

[16] M. V. Ramakrishna and R. A. Friesner, Phys. Rev. Lett. **67**, 629 (1991).

[17] G. T. Einevoll, Phys. Rev. B **45**, 3410 (1992).

[18] A. J. Kenyon, P. F. Trwoga, C. W. Pitt, and G. Rehm, J. Appl. Phys. **79**, 9291 (1996).

[19] A. J. Kenyon, P. F. Trwoga, and C. W. Pitt, Proc. Electrochem. Soc. **PV97-11**, 304 (1997).

[20] I. M. Lifshitz, Adv. Phys. **42**, 483 (1964).

[21] X. Chen, J. Zhao, G. Wang, and X. Shen, Phys. Lett. A **212**, 285 (1996).

[22] D. Zhang, R. M. Kolbas, P. D. Milewski, D. J. Lichtenwalner, A. I. Kingon, and J. M. Zavada, Appl. Phys. Lett. **65**, 2684 (1994).

[23] J. B. Khurgin, E. W. Forsythe, S. I. Kim, B. S. Sywe, B. A. Khan, and G. S. Tompa, Mater. Res. Soc. Symp. Proc. **358**, 193 (1995).

[24] G. Ghislotti, B. Nielson, P. Asoka-Kumar, K. G. Lynn, A. Gambhir, L. F. Di Mauro, and C. E. Bottani, J. Appl. Phys. **79**, 8660 (1996).

[25] P. F. Trwoga, A. J. Kenyon, and C. W. Pitt, Electron. Lett. **32**, 1703 (1996).